Translational Oncology 27 (2023) 101581

Contents lists available at ScienceDirect

Translational Oncology

journal homepage: www.elsevier.com/locate/tranon

N6-methyladenosine-related lncRNAs in combination with computational histopathology and radiomics predict the prognosis of bladder cancer

Ziye Huang [a], Guang Wang [a], Yuyun Wu [a], Tongxin Yang [a], Lishi Shao [b], Bowei Yang [a], Pei Li [a,*], Jiongming Li [a,*]

[a] The Department of Urology, The Second Affiliated Hospital of Kunming Medical University, No. 374 Dian-Mian Avenue, Kunming, Yunnan, 650101, P.R. China
[b] The Department of Imageology, The Second Affiliated Hospital of Kunming Medical University, No. 374 Dian-Mian Avenue, Kunming, Yunnan, 650101, P.R. China

ARTICLE INFO

Keywords:
Biomarker
Diagnosis
Radiomics
Urinary bladder neoplasms
Prognosis

ABSTRACT

Objectives: Identification of m6A- related lncRNAs associated with BC diagnosis and prognosis.
Methods: From the TCGA database, we obtained transcriptome data and corresponding clinical information (including histopathological and CT imaging data) for 408 patients. And bioinformatics, computational histopathology, and radiomics were used to identify and analyze diagnostic and prognostic biomarkers of m6A-related lncRNAs in BC.
Results: 3 significantly high-expressed m6A-related lncRNAs were significantly associated with the prognosis of BC. The BC samples were divided into two subgroups based on the expression of the 3 lncRNAs. The overall survival of patients in cluster 2 was significantly lower than that in cluster 1. The immune landscape results showed that the expression of PD-L1, T cells follicular helper, NK cells resting, and mast cells activated in cluster 2 were significantly higher, and naive B cells, plasma cells, T cells regulatory (Tregs), and mast cells resting were significantly lower. Computational histopathology results showed a significantly higher percentage of tumor-infiltrating lymphocytes (TILs) in cluster 2. The radiomics results show that the 3 eigenvalues of diagnostics image-original minimum, diagnostics image-original maximum, and original GLCM inverse variance are significantly higher in cluster 2. High expression of 2 bridge genes in the PPI network of 30 key immune genes predicts poorer disease-free survival, while immunohistochemistry showed that their expression levels were significantly higher in high-grade BC than in low-grade BC and normal tissue.
Conclusion: Based on the results of immune landscape, computational histopathology, and radiomics, these 3 m6A-related lncRNAs may be diagnostic and prognostic biomarkers for BC.

Introduction

N6-methyladenine (m6A) is the methylated adenosine at the N6 site, which is a wide and abundant modification in mRNA. By regulating RNA splicing, degradation, and translation, m6A methylation modification regulates various biological processes, including cell proliferation, metabolism, and metastasis, and these processes are also related to anticancer drug resistance [1]. In recent years, the research on m6A methylation modification related genes has been deepened, and the number of related genes has been found to be increasing. According to their regulatory function in m6A methylated modification, these genetic proteins are vividly classified into "writers," "erasers," and "readers" [2]. The "Writers" form multiple complexes centered on METTL3 and METTL14 proteins, which are correlated with each other and mainly promote the initial mRNA to undergo m6A methylation to form mature mRNA [1, 3, 4]. "Erasers" primarily remove the m6A methylation modification of mRNA [5–7]. "Readers'" main functions include the export, splicing, stabilization, translation, and decay of m6A methylated modified mRNA [3–10]. (Fig. 1)

Long non-coding RNAs (lncRNAs) are non-translated functional proteins with a length of more than 200 nucleotides that are produced during genome transcription. It is estimated that there are over 100,000

Abbreviations: BC, Bladder Cancer; m6A, N6-methyladenine; TCGA, The Cancer Genome Atlas; TILs, Tumor-Infiltrating Lymphocytes; OS, Overall Survival; GLCM, Gray-Level Co-occurrence Matrix; CT, Computerized Tomography; GO, Gene Ontology; KEGG, Kyoto Encyclopedia of Genes and Genomes; PPI, Protein-Protein Interaction.

* Corresponding author.
E-mail addresses: peilinli@live.cn (P. Li), jiongmingli@aliyun.com (J. Li).

https://doi.org/10.1016/j.tranon.2022.101581
Received 22 October 2021; Received in revised form 22 October 2022; Accepted 27 October 2022

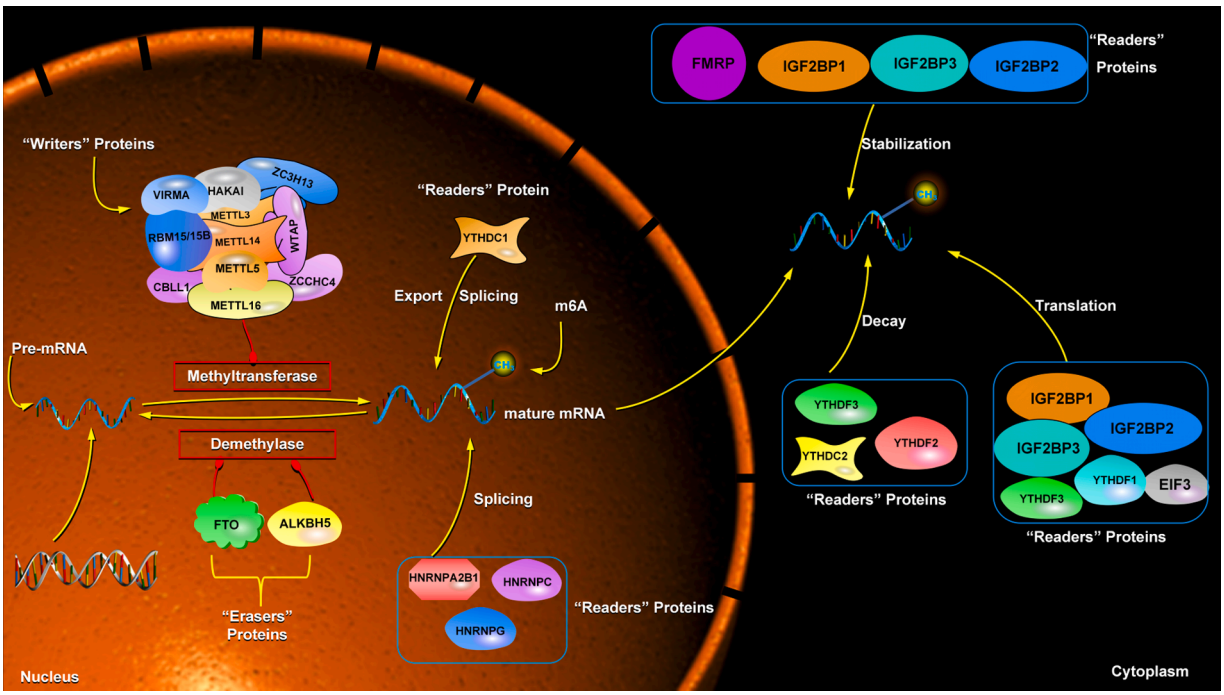

Fig. 1. The m6A methylation modulation of the "writers", "Erasers" and "readers" proteins in the mRNA. ZC3H13, HAKAI, VIRMA, METTL3, RBM15/15B, METTL14, WTAP, CBLL1, METTL5, ZCCHC4 and METTL16 of "writers" bind tightly or form complexes like "writers" that promote mRNA maturation and m6A methylation. FTO and ALKBH5 form a complex like "Erasers" that promotes m6A methylation of mRNA removal. And other proteins like "readers", the YTHDC1 splices the mRNA and exports the mature mRNA to the cytoplasm; HNRNPA2B1, HNRNPC and HNRNPG also have the effect of splicing mature mRNA; IGF2BP1, IGF2BP2, IGF2BP3, YTHDF1, YTHDF3 and EIF3 promotes mature mRNA translation; IGF2BP1, IGF2BP2, IGF2BP3 and FMRP maintain mature mRNA stabilization; YTHDF3, YTHDF2 and YTHDC2 promote mature mRNA decay.

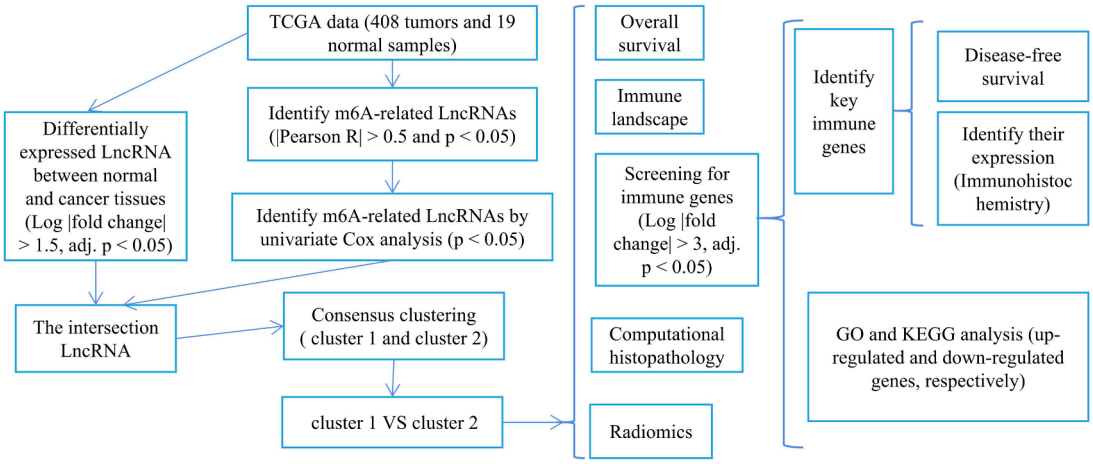

Fig. 2. Flow diagram.

human lncRNAs. Although the function of most lncRNAs is still unclear, there is sufficient evidence that an increasing number of lncRNAs have important functions. These include roles in gene regulation; influencing the expression of nearby genes, which in turn affects chromatin biology; as well as participating in different stages of mRNA, including splicing, conversion and translation, and signalling pathways. [11]

Studies have confirmed that m6A "writers", "readers" and "erasers" interact with lncRNAs to influence tumor initiation and progression [4]. Such as, lncRNA X-Inactive Specific transcript (XIST) is a modification of the methylation target of RBM15/RBM15B, acting directly on ZC3H13 that communicates with m6A. At the same time, RBM15/RBM15B, WTAP, and METTL3 form a complex that acts on XIST with WTAP as the interaction point [12]. LINC00632, resulting in CDR1-AS (cerebellar degeneration-associated 1 antisense) deletion, promotes melanoma invasion and metastasis through the regulation of the "reader" IGF2BP3 [13]. SOX2OT (SOX2 overlapping transcript) promotes the transcription of demethylated SOX2 through "eraser" ALKBH5, resulting in increased expression of SOX2 (SRY-box transcription factor 2), thereby inhibiting apoptosis, promoting cell proliferation, inhibiting glioblastoma resistance to temozolomide, and activating the Wnt5a/-catenin pathway. [14].

However, there are few clinical and experimental studies on the role of m6A-related lncRNAs in BC. Therefore, we used the TCGA database to screen the m6A-related lncRNAs in BC samples in this paper. Bioinformatics methods, computational histopathology, and radiomics analysis were used to discuss the relationship between m6A-related lncRNAs and

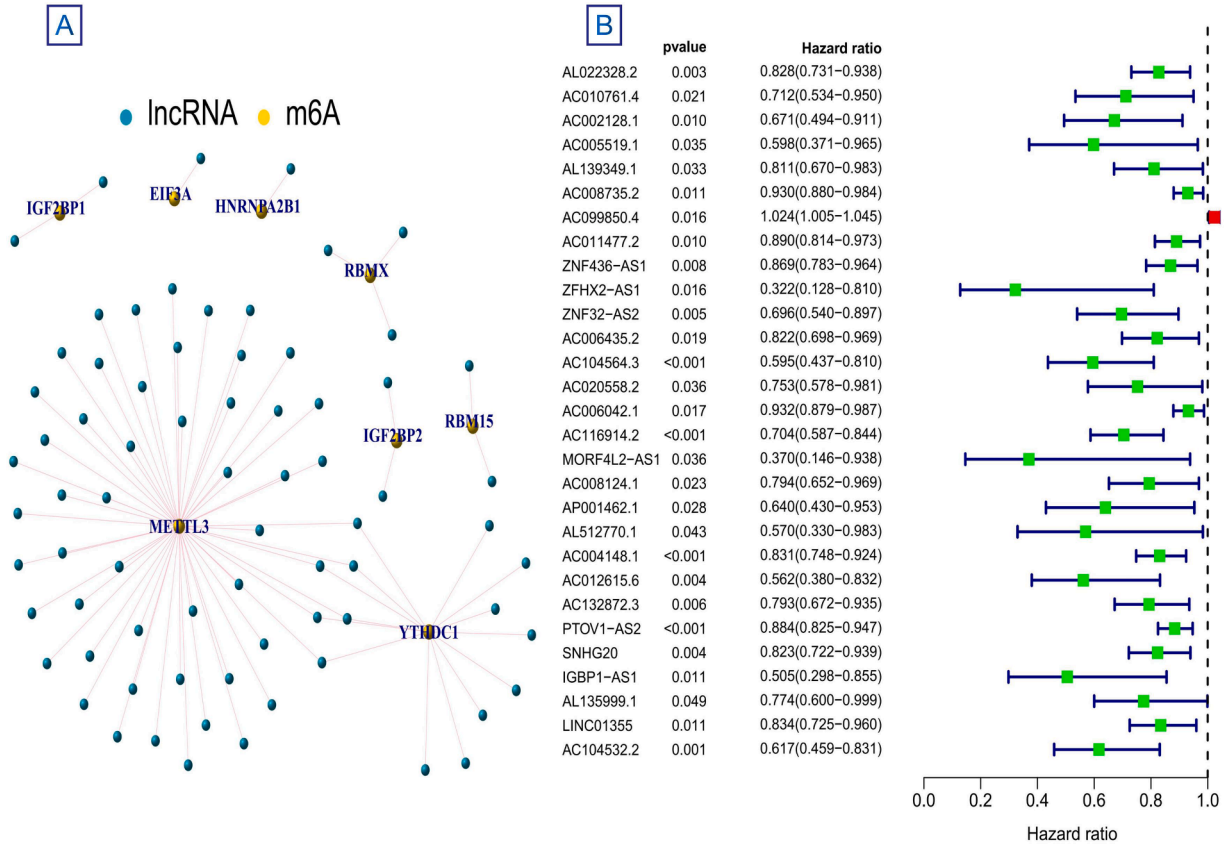

Fig. 3. (a) Screened m6A RNA methylation regulators ("writers", "Erasers" and "readers") interact with m6A-related lncRNAs networks. (b) The hazard ratio forest plots showed univariate Cox analysis screened 3 M6A-related prognostic lncRNAs.

the prognosis of BC. (Fig. 2).

Materials and methods

Sample data acquisition

The Cancer Genome Atlas (TCGA) database was used to obtain RNA-seq transcriptome, clinical characteristics, and computerized tomography (CT) images of BC patients. After removing duplicate samples, we included 408 tumors and 19 normal samples. And we downloaded tumor-infiltrating lymphocytes (TILs) percentage data and BC pathological images from The Cancer Imaging Archive (TCIA) database (https://cancerimagingarchive.net/datascope/TCGA_TilMap/home/).

M6A - related LncRNAs

The 27 relatively closely related genes (METTL3, METTL5, METTL14, METTL16, WTAP, RBM15, RBM15B, ZC3H13, KIAA1429/VIRMA, TRMT112, CBLL1, ZCCHC4, FTO, ALKBH5, YTHDC1, YTHDC2, YTHDF1, YTHDF2, YTHDF3, IGF2BP1, IGF2BP2, IGF2BP3, HNRNPC, EIF3/EIF3A, HNRNPG/RBMX, HNRNPA2B1, FMRP) were screened from the recently published literature [3, 10]. The human lncRNA annotation file was obtained from GENCODE (https://www.gencodegenes.org/); according to lncRNA annotation files, 14086 lncRNAs were screened by R software (version 4.0.5). In addition, lncRNAs and m6A co-expression networks were constructed using the “igraph” package (screening criteria:|Pearson’s R| $>$ 0.5 and p $<$ 0.05).

Prognostic M6A-related LncRNAs screening

The "survival" package was used to screen for prognostic m6A-related lncRNAs (P-value filter $<$ 0.05). Then, the differentially expressed LncRNAs between normal and cancer tissues were screened (Log |fold change| $>$ 1.5, adj. p $<$ 0.05), and the intersection with prognostic m6A-related lncRNAs was also screened. Forest plots were then generated by univariate cox analysis of lncRNA data. In addition, the "pheatmap" package was used to map the expression levels of lncRNAs with significant prognostic value in tumor and normal samples.

Bioinformatics analysis

We used the "ConsensusClusterPlus" package to classify bladder cancer into subtypes based on prognostically relevant lncRNAs (1000 iterations, 80% resampling rate). Overall survival (OS) of different subtypes was analyzed using the "Survival" package, and survival curves were drawn using the Kaplan-Meier method. The "pheatmap" package was used to visualize the relationship between prognostic lncRNA expression and clinicopathological features. The "CIBERSORT" algorithm calculates the immune infiltration of BC samples and visualizes it with the "vioplot" package. Differences in expression among TILs, immune cells, PD-L1 and PD-1 subsets were then analyzed using the "limma" package and visualized using the "ggpubr" package. GO (Gene

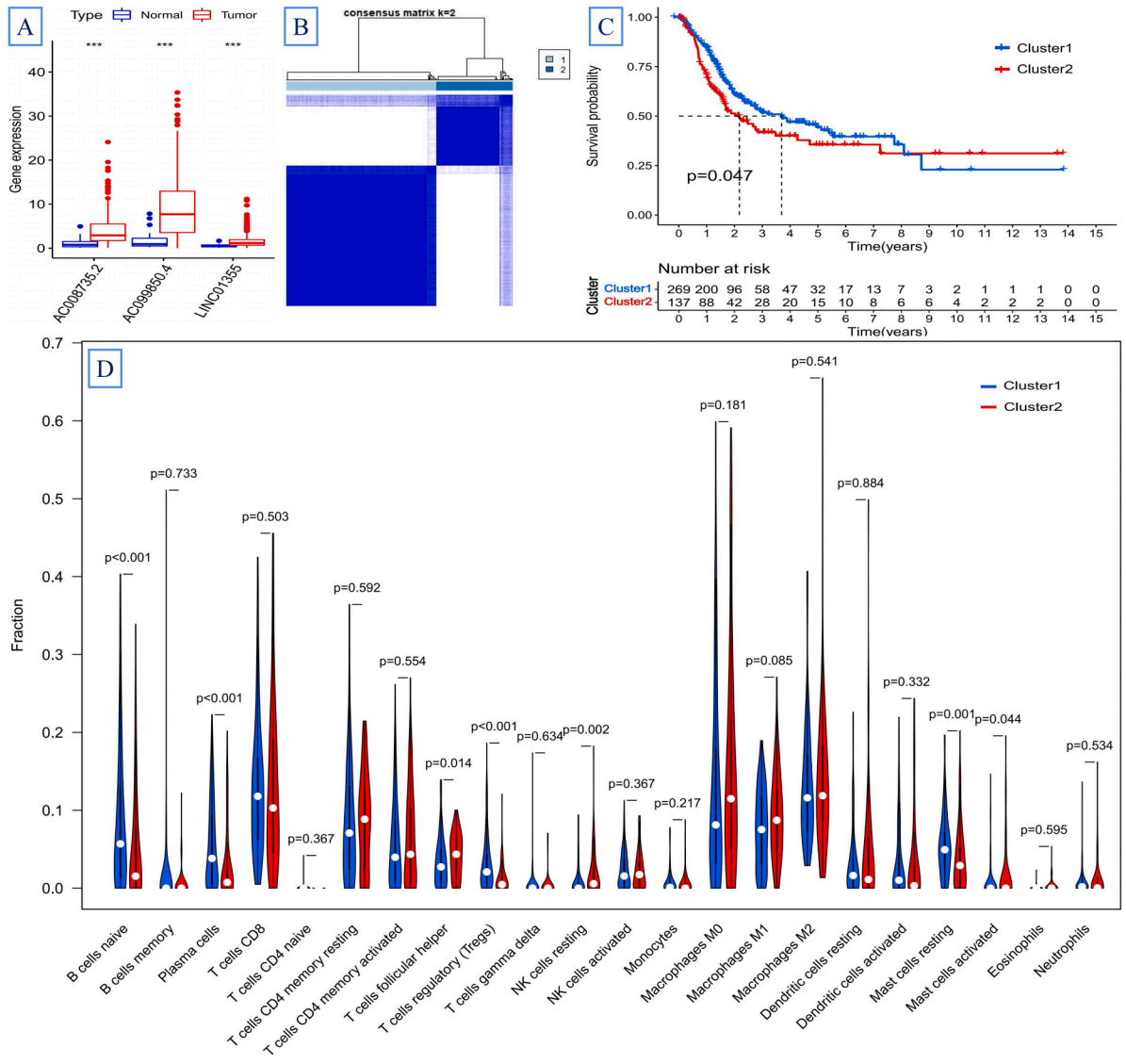

Fig. 4. (a) Differential expression of 3 m6A-related prognostic lncRNAs in bladder cancer and normal bladder tissue (* $p < 0.05$, ** $p < 0.01$, and *** $p < 0.001$). Consensus cluster analysis was performed on 3 M6A-related Prognostic lncRNAs in 408 bladder cancer samples, (b) Consensus clustering matrix for $k = 2$, (c) The survival analysis for the two clusters by Kaplan-Meier method. (d) Differences in the abundance of 22 immune cell types between cluster 1 and cluster 2 in bladder cancer.

Ontology) and KEGG (Kyoto Encyclopedia of Genes and Genomes) enrichment analyses were performed on up-regulated and down-regulated immune genes between subgroups by "org.Hs.eg.db", respectively. Finally, the PPI (Protein-Protein Interaction) analysis of differential immune genes was performed using online tools and the 30 key genes were obtained by Cytoscape software (MCC algorithm of cytoHubba).

Radiomics

A professor in the urology department and a doctor in the imaging department jointly read the patient's CT and used 3D Slier (Version 4.11) image processing software to mark the BC in the CT. After processing, the "radiomics" package in Python (Version 3.7) software was used to identify tumour sites and extract characteristics (such as density, size, greyscale, etc.) from CT images, and the features with significant statistical significance between subgroups were screened ($P < 0.05$).

Bridging immune gene immunohistochemistry and disease-free survival

Among the top 30 key immune genes analyzed by Cytoscape software, we searched for bridge genes, analyzed their influence on disease-free survival of patients, and observed their expression in tumor and normal tissues by immunohistochemistry. Disease-free survival analysis from GEPIA2 (http://gepia2.cancer-pku.cn/#survival), immunohistochemistry from The Human Protein Atlas (https://www.proteinatlas.org/).

Table 1
Differences in clinical characteristics between Cluster 1 and Cluster 2.

Clinical characteristics	Cluster1 (N=272)	Cluster2 (N=136)	P
Gender			0.111
Male	194 (71.3%)	107 (78.7%)	
Female	78 (28.7%)	29 (21.3%)	
Age (years)			0.381
≤60	75 (27.6%)	32 (23.5%)	
>60	197 (72.4%)	104 (76.5%)	
Grade			0.005
High	251 (92.3%)	133 (97.8%)	
Low	20 (7.3%)	1 (0.7%)	
Unknow*	1 (0.4%)	2 (1.5%)	
TNM stage			0.644
I	1 (0.4%)	1 (0.7%)	
II	92 (33.8%)	38 (28.0%)	
III	92 (33.8%)	48 (35.3%)	
IV	86 (31.6)	48 (35.3%)	
Unknow*	1 (0.4%)	1 (0.7%)	
T			0.463
T0	0 (0%)	1 (0.7%)	
T1	1 (0.4%)	2 (1.5%)	
T2	80 (29.4%)	39 (28.7%)	
T3	129 (47.4%)	65 (47.8%)	
T4	39 (14.3%)	19 (14.0%)	
TX*	1 (0.4%)	0 (0%)	
Unknow*	22 (8.1%)	10 (7.3%)	
M			0.918
M0	137 (50.4%)	59(43.4%)	
M1	7 (2.5%)	4 (3.0%)	
MX*	127 (46.7%)	71 (52.2%)	
Unknow*	1 (0.4%)	2 (1.4%)	
N			0.307
N0	159 (58.4%)	78 (57.4%)	
N1	26 (9.6%)	20 (14.7%)	
N2	53 (19.5%)	22 (16.2%)	
N3	4 (1.5%)	4 (2.9%)	
NX*	25 (9.2%)	11 (8.1%)	
Unknow*	5 (1.8%)	1 (0.7%)	

The P value is chi-square test result, * means not included in the statistical test.

Results

prognostic m6A - related lncRNAs identified

According to the filter conditions (|Pearson R| > 0.5 and p < 0.05), the results showed that 8 m6As were associated with 79 lncRNAs (Fig. 3a and Supplementary Tables S1–S2). Then, univariate cox regression analysis was used to identify prognosis-related lncRNAs, obtaining 29 lncRNAs (Fig. 3b and Supplementary Tables S1–S2). Finally, it intersected with significantly differentially expressed lncRNAs to produce 3 (AC008735.2, AC099850.4, and LINC01355) up-regulated, prognostically m6A-associated lncRNAs. (Fig. 4a).

Consensus clustering subgroup analysis

Samples were classified according to the expression levels of 3 prognostic lncRNAs using a consensus clustering method (K = 2 to 9). When k = 2, showing the best classification, 408 samples were divided into clusters 1 and 2 (Fig. 4b). The OS rate of cluster 2 patients was significantly lower than that of cluster 1 (Fig. 4c, P = 0.047). In addition, cluster 2 has more high-grade patients (Table 1, Fig. 5a, P = 0.005).

Immune landscape

Analysis of subgroup immunity revealed that the percentage of TILs (Fig. 6a, p = 0.004) was significantly higher in cluster 2. The results of immune cell infiltration revealed that naive B cells (p < 0.001), plasma cells (p < 0.001), T cells regulatory (Tregs) (p < 0.001), and mast cells resting (p < 0.001) were found in cluster 1 higher infiltration (Fig. 6b, c, f and g), while T cells follicular helper (p = 0.034), NK cells resting (p < 0.001) and mast cells activated (p = 0.001) were shown in cluster 2 higher infiltration (Fig. 6 d, e and h). The immune checkpoint PD-L1 was significantly overexpressed in cluster 2, while PD-1 was not statistically significant (Fig. 5 b and c, p < 0.001).

PPI, GO and KEGG

PPI showed that 27 down-regulated immune genes were closely related to 63 up-regulated immune genes (Fig. 8a), and Cytoscape software screened 30 key genes (Fig. 9a).

GO analysis showed that the main enriched biological processes (BP) of up-regulated genes were regulation of innate immune response, regulation of response to biotic stimulus, positive regulation of defense response, etc.; the enriched cellular components (CC) were vesicle lumen, secretory granule lumen, cytoplasmic vesicle lumen, etc.; the enriched molecular functions (MF) were ubiquitin-like protein ligase binding, cadherin binding, receptor ligand activity, etc. (Fig. 8c and supplementary material Table S4). The main enriched BP of down-regulated genes were regulation of MAP kinase activity, positive regulation of lymphocyte activation, positive regulation of leukocyte activation, etc.; enriched CC were collagen-containing extracellular matrix, secretory granule lumen, cytoplasmic vesicle lumen, etc.; enriched MF were receptor ligand activity, signaling receptor activator activity, growth factor activity, etc. (Fig. 8b and supplementary material Table S5).

The KEGG results of 30 key immune genes showed that the main enriched pathways included proteoglycans in cancer, MAPK signaling pathway, PI3K-Akt signaling pathway, chemokine signaling pathway, PD-L1 expression and PD-1 checkpoint pathway in cancer, etc. (Supplementary material Table S6)

Radiomics

CT tumor site features were extracted from 106 patients (70 in group 1 and 36 in group 2). Finally, 109 eigenvalues were extracted, of which 3 eigenvalues (diagnostics_Image-original_Minimum (P = 0.026), diagnostics_Image -original_Maximum (P = 0.022) and original_glcm_InverseVariance (P = 0.013)) were higher in cluster 2 (Fig. 7).

Bridging immune gene immunohistochemistry and disease-free survival

Cytoscape software identified 30 key immune genes with significant differences, among which HSP90AA1 and PAK2 were bridges in the PPI network (Fig. 9 a), and the Pearson's test showed that they were significantly correlated (Fig. 9 e, correlation coefficient R = 0.49, p < 0.001). Disease-free survival analysis showed that the survival of HSP90AA1 and PAK2 in the high-expression group was significantly lower than that in the low-expression group (Fig. 9 c and d, p = 0.007 and p = 0.010). Immunohistochemical results showed that HSP90AA1 and PAK2 were significantly expressed in high-grade BC, while in low-grade BC and normal tissue expression is not obvious (Fig. 9 b).

Discussion

BC ranks among the top 10 malignancies, causing approximately 165,000 deaths annually [15]. Although surgery can remove the primary lesion, the recurrence rate is high. The 5-year recurrence rate of non-muscle-invasive BC after TUR alone is as high as 58.8%, and the recurrence rate is 35 % even after adjuvant chemotherapy [16]. For patients with middle and advanced stages, such as radical cystectomy and urinary diversion, patients must bear financial pressure and maintain psychological pressure. Although immunotherapy for BC has entered the clinic, ideal immune targets are still being explored. M6A is the most common nucleotide modification in mRNA. More and more studies have confirmed that m6A-related enzymes play an important role in the occurrence and development of BC, such as METTL3, which

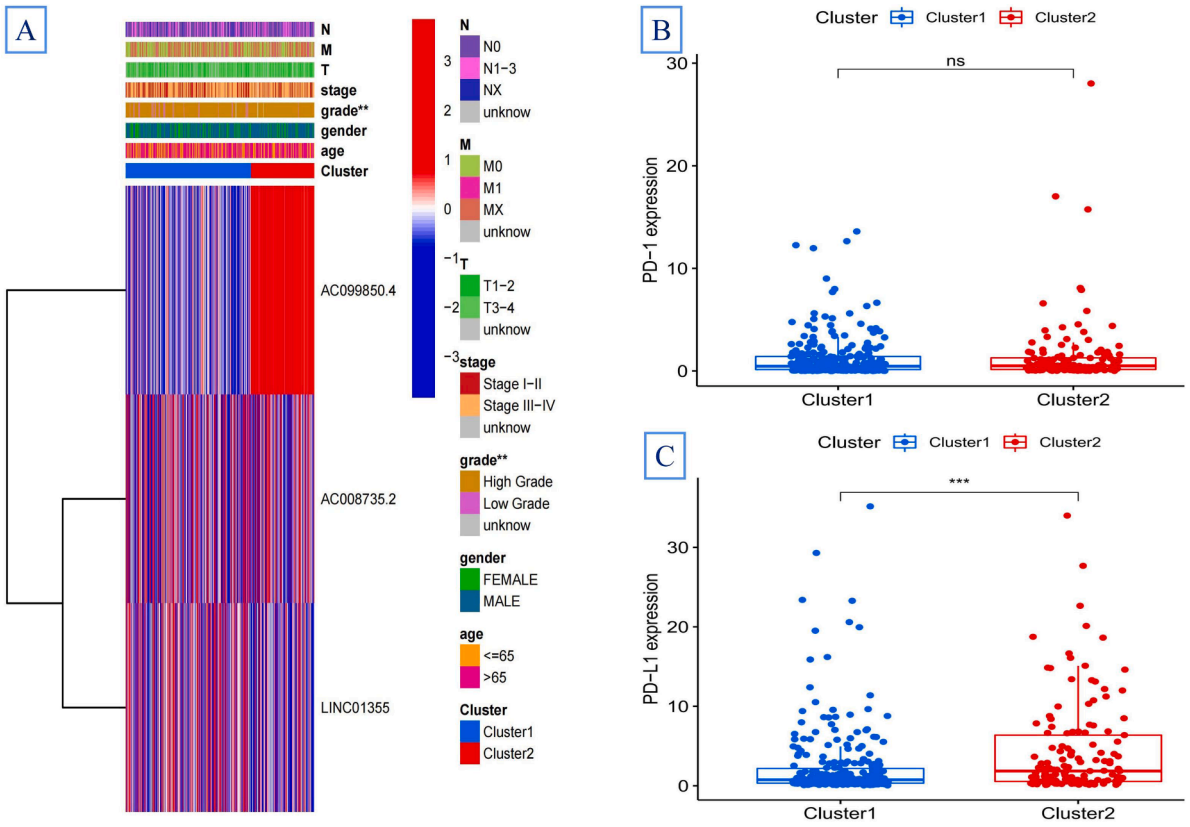

Fig. 5. (a) The heatmap shows the expression, and clinicopathological characteristics distribution and statistical differences of 3 lncRNAs (AC008735.2, AC099850.4 and LINC01355) in cluster 1 and cluster 2. (b and c) The expression of immune checkpoint PD-L1 and PD-1 in cluster 1 and cluster 2. (ns means $P > 0.05$, ** means $P < 0.01$, *** means $P < 0.001$)

positively regulates pri-mir221/222 in an m6A-dependent manner and plays a carcinogenic role in BC [17]. METTL14 inhibits the self-renewal and tumorigenesis of BC initiating cells by Notch1′s N (6) -methyladenosine [18]. LncRNAs are non-translated RNAs over 200 nucleotides in length that were previously thought to have no biological function. However, with the progress of research, more and more studies have confirmed that lncRNAs play a role in gene regulatory mechanisms, including mRNAs and signaling pathways involved in different stages [11]. A growing number of studies have found that lncRNAs are associated with BC size, metastasis, invasion and drug resistance [19].

Few studies have shown that m6A-related lncRNAs are closely related to the progression of BC. Through bioinformatics, we identified 3 m6A-related lncRNAs that were significantly overexpressed and significantly correlated with patient prognosis. Our consensus clustering analysis of these 3 lncRNAs identified two subtypes: cluster 1 (including 272 patients) and cluster 2 (including 136 patients). Survival analysis showed that the OS rate of cluster 2 patients was significantly lower than that of cluster 1, and the clinicopathological grade was significantly higher in cluster 2. The immune landscape results showed that the expression of PD-L1, TILs, T cells follicular helper, NK cells resting, and mast cells activated was significantly higher in cluster 2, while naive B cells, plasma cells, T cells regulatory (Tregs), and mast cells resting were significantly lower. Studies have shown that the expression of the PD-1/PD-L1 checkpoint can inhibit tumor-induced B cell and T cell immunity and macrophage phagocytosis [20–22], and inhibition of PD-L1 can aggregate and activate T cells, B cells, and macrophages [23]. A subset of native plasma cells can express inhibitory receptors for PD-L1 and PD-L2 [24]. NK cells are anti-tumor innate immune cells that can inhibit the progression and recurrence of BC [25]. The role of mast cells in BC is unclear, but it has been reported that mast cell density is significantly higher in high-grade BC than in low-grade [26].

We analyzed the immune genes of cluster 2 and cluster 1, and performed GO analysis on up-regulated and down-regulated genes, respectively. It was found that up-regulated genes were mainly enriched in regulation of innate immune response, regulation of response to biotic stimulus, positive regulation of defense response, etc., while down-regulated genes were mainly enriched in regulation of MAP kinase activity, positive regulation of lymphocyte activation, positive regulation of leukocyte activation, et al. Interestingly, the down-regulated immunity in cluster 2 was mainly enriched in the activation of immune pathways, implying that the high tumor grade in cluster 2 was due to the silencing of genes of these immune activation pathways. Then, 30 key genes in differentially expressed immune genes were clustered, and they were found to be proteoglycans in cancer, MAPK signaling pathway, PI3K-Akt signaling pathway, chemokine signaling pathway, PD-L1 expression, and PD-1 checkpoint pathway in cancer, etc. indicate that these pathways are responsible for tumor progression in cluster 2. We noted that HSP90AA1 and PAK2 were bridge proteins of the PPI network, and found that their high expression was significantly associated with low disease-free survival, and immunohistochemistry showed that their expression was significantly higher in high-grade BC than in low-grade and normal bladder tissue. Related studies have shown that

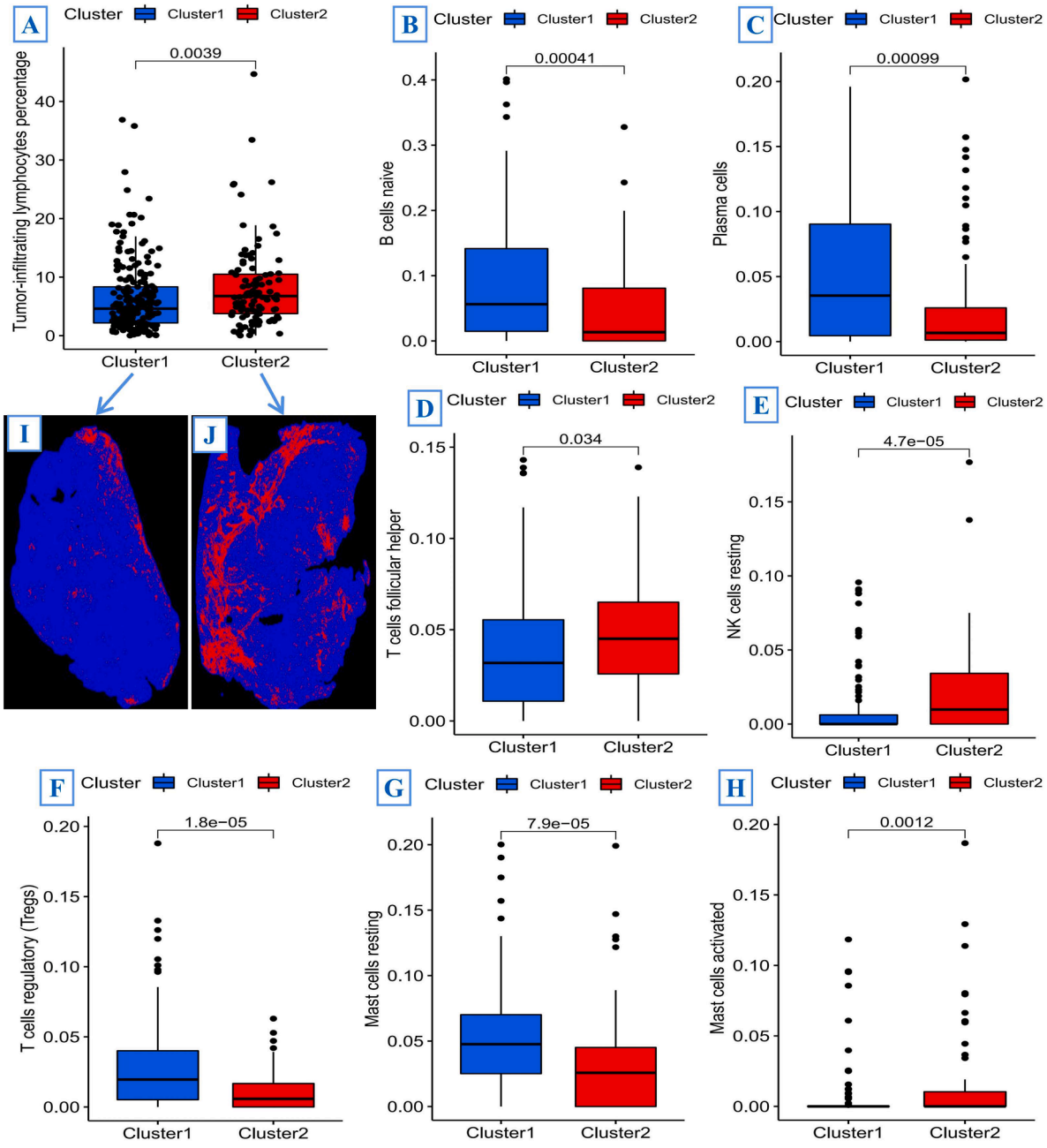

Fig. 6. (a) Tumor-infiltrating lymphocytes (TILs) percentage in Cluster 1 and Cluster 2 (Figure i and j respectively represent the computational histopathology processed maps of the two cluster groups, and the red spots represent TILs). (b, c, d, e, f, g and h) 7 types of immune cells (B cells naïve, Plasma cells, T cells follicular helper, NK cells resting, T cells regulatory (Tregs), Mast cells resting, and Mast cells activated were significantly different in cluster 1 and cluster 2.

HSP90AA1 [27–29] and PAK2 [30–32] promote tumor progression, but there are few studies in BC.

Computational histopathology refers to transforming pathological images into high-fidelity and high-throughput mining data based on artificial intelligence, which is used to quantify pathological diagnosis and disease prognosis and automatically generate pathological diagnosis reports [33]. Radiomics refers to the high-throughput extraction of a large amount of image information from images (CT, MRI, PET, etc.), and the analysis of image data information to help doctors make the most accurate diagnosis [34]. Our study of computational histopathology data found that TILs significantly associated with the prognosis of urologic tumors [35] in cluster 2 were significantly higher than those in cluster 1, and many studies showed a correlation between TILs diagnosis and treatment of tumors [36]. Furthermore, among the 109 features extracted from radiomics, the eigenvalues of diagnostics_Image-original_Minimum, diagnostics_Image -original_Maximum, and original_glcm_InverseVariance were significantly higher in cluster 2. In short, the above-mentioned discovery of

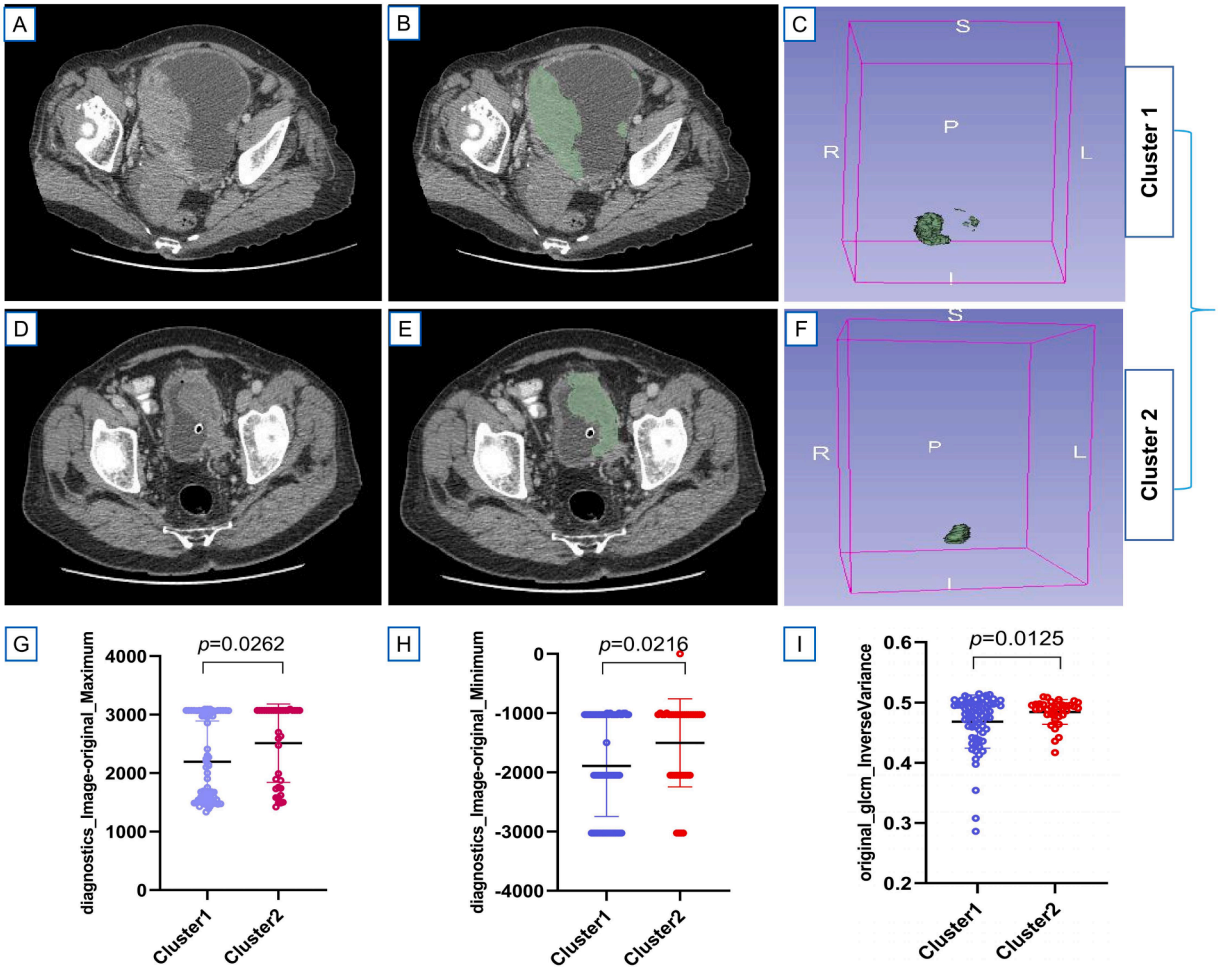

Fig. 7. (a, b) Radiomics performed marking and characteristic extraction on each layer of CT images of cluster 1 and cluster 2. (a, b, c, d, e and f) The process from the marking of each slice of CT to the formation of a 3D map of the bladder tumor. (g, h and i) 3 characteristics have significant significance in cluster 1 and cluster 2.

m6A-related lncRNAs provides a new target for BC diagnosis and therapy.

Conclusion

In this paper, two subtypes of m6A-related lncRNAs in BC were analyzed from RNA-omics, computational histopathology, and radiomics. Significant differences were found between the two subtypes in clinical, immunological, pathological, and CT features, which were closely related to the prognosis of BC. In a word, we provide biological targets and multi-omics approaches for diagnosing and treating BC.

Authors' contributions

All authors read and approved the final version of the manuscript. Ziye Huang Data analysis and manuscript writing; Guang Wang and Yuyun Wu Revised draft; Pei Li and Tongxin Yang Revised draft, Manuscript editing and formal analysis; Bowei Yang Data collection; Lishi Shao and Jiongming Li CT processing and review manuscript.

Funding

This study was supported by Grant No. 82160150 from the National Natural Science Foundation of China, and Grant No. 2019FE001(-149), No. 202001AY070001-062 and No. 202101AY070001-154 from the Yunnan Provincial Science and Technology Department / Kunming Medical University Joint Project of Basic Research, and Grant No. 202201AT070240 from the Basic Research Project of Yunnan Provincial Science and Technology Department, and Grant No. H-2017045 from the Medical Science Specialist Training Project of Yunnan Provincial Health Commission, and Grant No. 202105AF150063 from the Yunnan Provincial Science and Technology Department Zhangqun Ye Expert's Workstation.

Availability of data and materials

Transcriptome profiling raw data with corresponding clinical information were downloaded from TCGA (https://cancergenome.nih.gov/) and the TCIA (https://cancerimagingarchive.net/datascope/TCGA_TilMap/home/) databases.

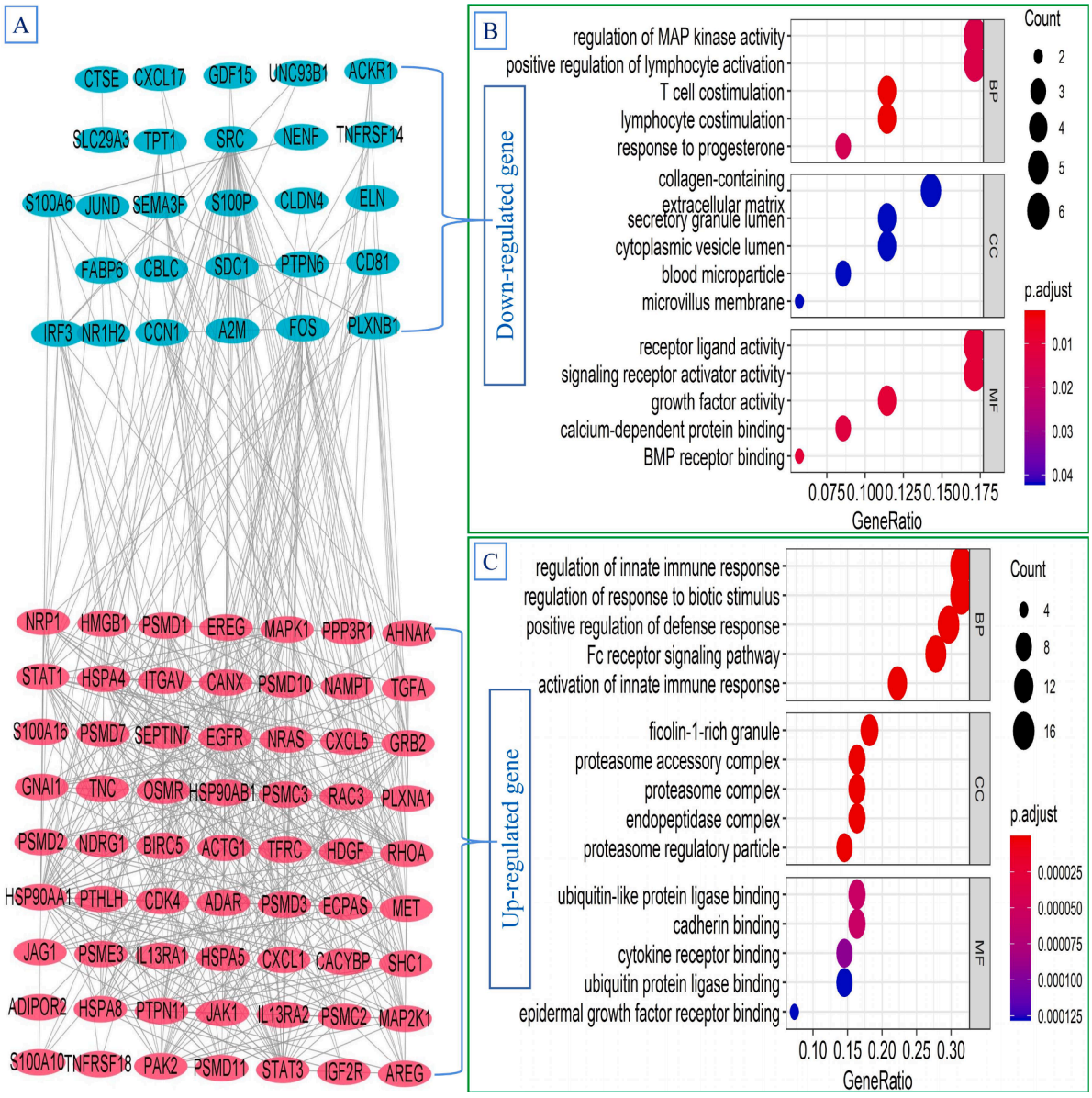

Fig. 8. (a) Immune-related genes significantly different between cluster1 and cluster2 (green and red represent low and high expressed genes in Cluster2 group, respectively). (b and c) GO (Gene Ontology) enrichment analysis of low and high expressed genes (BP=Biological Process, CC=Cellular Component, MF=Molecular Function).

Ethics approval and consent to participate

Not applicable.

Consent for publication

Not applicable.

Footnotes

Ziye Huang, Guang Wang and Yuyun Wu contributed equally to this work.

Author contribution statement

All authors read and approved the final version of the manuscript. Ziye Huang Data analysis and manuscript writing; Guang Wang and Yuyun Wu Revised draft; Pei Li and Tongxin Yang Revised draft, Manuscript editing and formal analysis; Bowei Yang Data collection; Lishi Shao and Jiongming Li CT processing and review manuscript.

Declaration of Competing Interest

The authors have declared that no competing interest exists.

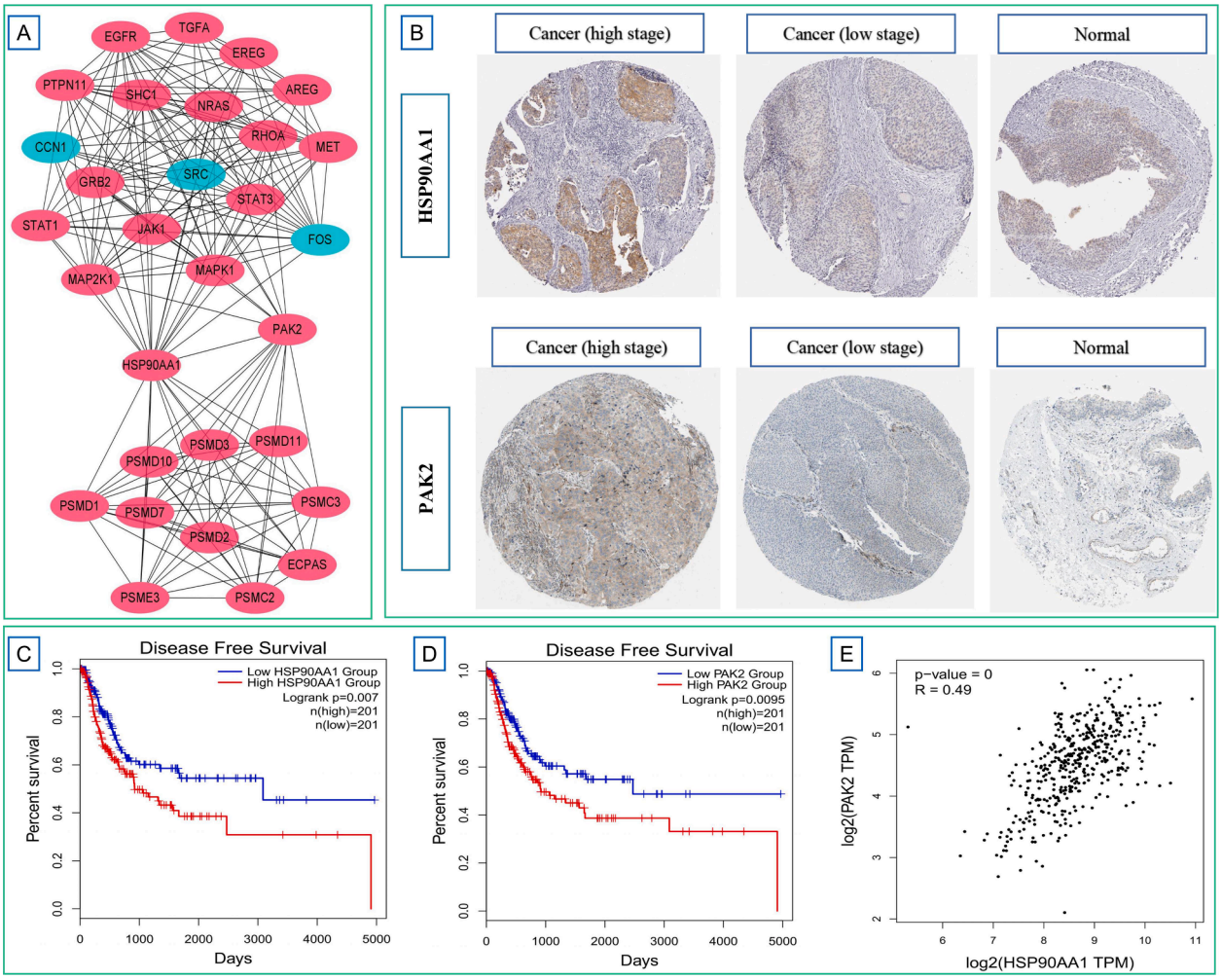

Fig. 9. (a) 30 key gene interaction results obtained by Cytoscape software (MCC algorithm of cytoHubba, green and red represent genes with low and high expression, respectively). (b) Immunohistochemical results, the expression of HSP90AA1 and PAK2 in bladder cancer and normal tissues. (c and d) Disease-free survival between high and low expression groups of HSP90AA1 and PAK2. (e) Pearson correlation between HSP90AA1 and PAK2 expression (Correlation Coefficient R =0.49, P < 0.001).

Supplementary materials

Supplementary material associated with this article can be found, in the online version, at doi:10.1016/j.tranon.2022.101581.

References

[1] B Li, J Jiang, YG Assaraf, H Xiao, ZS Chen, C. Huang, Surmounting cancer drug resistance: New insights from the perspective of N(6)-methyladenosine RNA modification, Drug Resist. Updat. 53 (2020), 100720.

[2] Y Fu, D Dominissini, G Rechavi, C. He, Gene expression regulation mediated through reversible m^{6}A RNA methylation, Nat. Rev. Genet. 15 (5) (2014) 293–306.

[3] S Zaccara, RJ Ries, SR. Jaffrey, Reading, writing and erasing mRNA methylation, Nat. Rev. Molecul. Cell Biol. 20 (10) (2019) 608–624.

[4] D Dai, H Wang, L Zhu, H Jin, X. Wang, N6-methyladenosine links RNA metabolism to cancer progression, Cell Death. Dis. 9 (2) (2018) 124.

[5] Z Zhou, J Lv, H Yu, J Han, X Yang, D Feng, et al., Mechanism of RNA modification N6-methyladenosine in human cancer, Mol. Cancer 19 (1) (2020) 104.

[6] Y Lee, J Choe, OH Park, YK. Kim, Molecular mechanisms driving mRNA degradation by m(6)A modification, Trend. Genet. 36 (3) (2020) 177–188.

[7] Y Chen, Y Lin, Y Shu, J He, W. Gao, Interaction between N(6)-methyladenosine (m (6)A) modification and noncoding RNAs in cancer, Mol. Cancer 19 (1) (2020) 94.

[8] ZM Zhu, FC Huo, DS. Pei, Function and evolution of RNA N6-methyladenosine modification, Int. J. Biol. Sci. 16 (11) (2020) 1929–1940.

[9] W Zhao, X Qi, L Liu, S Ma, J Liu, J. Wu, Epigenetic regulation of m(6)A modifications in human cancer, Molecul. Ther. Nucl. Acid. 19 (2020) 405–412.

[10] T Wang, S Kong, M Tao, S. Ju, The potential role of RNA N6-methyladenosine in cancer progression, Mol. Cancer 19 (1) (2020) 88.

[11] L Statello, CJ Guo, LL Chen, M. Huarte, Gene regulation by long non-coding RNAs and its biological functions, Nat. Rev. Molecul. Cell Biol. 22 (2) (2021) 96–118.

[12] Y Lan, B Liu, H. Guo, The role of M(6)A modification in the regulation of tumor-related lncRNAs, Molecul. Ther. Nucl. Acid. 24 (2021) 768–779.

[13] D Hanniford, A Ulloa-Morales, A Karz, MG Berzoti-Coelho, RS Moubarak, B Sánchez-Sendra, et al., Epigenetic silencing of CDR1as drives IGF2BP3-mediated melanoma invasion and metastasis, Cancer Cell 37 (1) (2020) 55–70.e15.

[14] B Liu, J Zhou, C Wang, Y Chi, Q Wei, Z Fu, et al., LncRNA SOX2OT promotes temozolomide resistance by elevating SOX2 expression via ALKBH5-mediated epigenetic regulation in glioblastoma, Cell Death. Dis. 11 (5) (2020) 384.

[15] DT Miyamoto, KW Mouw, FY Feng, WU Shipley, JA. Efstathiou, Molecular biomarkers in bladder preservation therapy for muscle-invasive bladder cancer, Lancet Oncol. 19 (12) (2018) e683–ee95.

[16] RJ Sylvester, W Oosterlinck, S Holmang, MR Sydes, A Birtle, S Gudjonsson, et al., Systematic review and individual patient data meta-analysis of randomized trials comparing a single immediate instillation of chemotherapy after transurethral resection with transurethral resection alone in patients with stage pta-pt1 urothelial carcinoma of the bladder: which patients benefit from the instillation? Eur. Urol. 69 (2) (2016) 231–244.

[17] J Han, JZ Wang, X Yang, H Yu, R Zhou, HC Lu, et al., METTL3 promote tumor proliferation of bladder cancer by accelerating pri-miR221/222 maturation in m6A-dependent manner, Mol. Cancer 18 (1) (2019) 110.

[18] C Gu, Z Wang, N Zhou, G Li, Y Kou, Y Luo, et al., Mettl14 inhibits bladder TIC self-renewal and bladder tumorigenesis through N(6)-methyladenosine of Notch1, Mol. Cancer 18 (1) (2019) 168.

[19] HJ Li, X Gong, ZK Li, W Qin, CX He, L Xing, et al., Role of long non-coding RNAs on bladder cancer, Front. Cell Dev. Biol. 9 (2021), 672679.

[20] A Goodman, SP Patel, R. Kurzrock, PD-1-PD-L1 immune-checkpoint blockade in B-cell lymphomas, Nat. Rev. Clin. Oncol. 14 (4) (2017) 203–220.

[21] F Dammeijer, M van Gulijk, EE Mulder, M Lukkes, L Klaase, T van den Bosch, et al., The PD-1/PD-L1-checkpoint restrains T cell immunity in tumor-draining lymph nodes, Cancer Cell 38 (5) (2020) 685–700.e8.

[22] SR Gordon, RL Maute, BW Dulken, G Hutter, BM George, MN McCracken, et al., PD-1 expression by tumour-associated macrophages inhibits phagocytosis and tumour immunity, Nature 545 (7655) (2017) 495–499.
[23] J Bellmunt, T Powles, NJ. Vogelzang, A review on the evolution of PD-1/PD-L1 immunotherapy for bladder cancer: the future is now, Cancer Treat. Rev. 54 (2017) 58–67.
[24] AC Lino, VD Dang, V Lampropoulou, A Welle, J Joedicke, J Pohar, et al., LAG-3 inhibitory receptor expression identifies immunosuppressive natural regulatory plasma cells, Immunity 49 (1) (2018) 120. -33.e9.
[25] D Ranti, C Bieber, YS Wang, JP Sfakianos, A. Horowitz, Natural killer cells: unlocking new treatments for bladder cancer, Trend. Cancer 8 (8) (2022) 698–710.
[26] JH Kim, YJ Kang, DS Kim, CH Lee, YS Jeon, NK Lee, et al., The relationship between mast cell density and tumour grade in transitional cell carcinoma of the bladder, J. Int. Med. Res. 39 (5) (2011) 1675–1681.
[27] Q Cheng, JT Chang, J Geradts, LM Neckers, T Haystead, NL Spector, et al., Amplification and high-level expression of heat shock protein 90 marks aggressive phenotypes of human epidermal growth factor receptor 2 negative breast cancer, Breast Cancer Res. 14 (2) (2012) R62.
[28] X Xiao, W Wang, Y Li, D Yang, X Li, C Shen, et al., HSP90AA1-mediated autophagy promotes drug resistance in osteosarcoma, J. Exp. Clin. Cancer Res. 37 (1) (2018) 201.
[29] M Zhang, Y Peng, Z Yang, H Zhang, C Xu, L Liu, et al., DAB2IP down-regulates HSP90AA1 to inhibit the malignant biological behaviors of colorectal cancer, BMC Cancer 22 (1) (2022) 561.
[30] H Liu, SH Shin, H Chen, T Liu, Z Li, Y Hu, et al., CDK12 and PAK2 as novel therapeutic targets for human gastric cancer, Theranostics 10 (14) (2020) 6201–6215.
[31] A Gupta, A Ajith, S Singh, RK Panday, A Samaiya, S. Shukla, PAK2-c-Myc-PKM2 axis plays an essential role in head and neck oncogenesis via regulating Warburg effect, Cell Death. Dis. 9 (8) (2018) 825.
[32] TY Cheng, YC Yang, HP Wang, YW Tien, CT Shun, HY Huang, et al., Pyruvate kinase M2 promotes pancreatic ductal adenocarcinoma invasion and metastasis through phosphorylation and stabilization of PAK2 protein, Oncogene 37 (13) (2018) 1730–1742.
[33] A Madabhushi, G. Lee, Image analysis and machine learning in digital pathology: challenges and opportunities, Med. Image Anal. 33 (2016) 170–175.
[34] P Lambin, RTH Leijenaar, TM Deist, J Peerlings, EEC de Jong, J van Timmeren, et al., Radiomics: the bridge between medical imaging and personalized medicine, Nat. Rev. Clin. Oncol. 14 (12) (2017) 749–762.
[35] M Miyake, S Hori, T Owari, Y Oda, Y Tatsumi, Y Nakai, et al., Clinical impact of tumor-infiltrating lymphocytes and PD-L1-positive cells as prognostic and predictive biomarkers in urological malignancies and retroperitoneal sarcoma, Cancers 12 (11) (2020).
[36] S Wang, J Sun, K Chen, P Ma, Q Lei, S Xing, et al., Perspectives of tumor-infiltrating lymphocyte treatment in solid tumors, BMC Med. 19 (1) (2021) 140.